

# Determination of mechanical and hydraulic properties of PVA hydrogels



Katarzyna Kazimierska-Drobny<sup>a,\*</sup>, Mirosława El Fray<sup>b</sup>, Mariusz Kaczmarek<sup>a</sup>

<sup>a</sup> Institute of Mechanics and Applied Computer Science, Kazimierz Wielki University, Kopernika 1, 85-074 Bydgoszcz, Poland

<sup>b</sup> Polymer Institute, West-Pomeranian University of Technology, Pulaskiego 10, 70-322 Szczecin, Poland

## ARTICLE INFO

### Article history:

Received 15 May 2014

Received in revised form 7 October 2014

Accepted 10 November 2014

Available online 12 November 2014

### Keywords:

PVA hydrogel

Creep test

Parameter identification

Young's modulus

Poisson's ratio

Permeability

## ABSTRACT

In this paper the identification of mechanical and hydraulic parameters of poly(vinyl alcohol) (PVA) hydrogels is described. The identification method follows the solution of inverse problem using experimental data from the unconfined compression test and the poroelastic creep model. The sensitivity analysis of the model shows significant dependence of the creep curves on investigated parameters. The hydrogels containing 22% PVA and 25% PVA were tested giving: the drained Young's modulus of 0.71 and 0.9 MPa; the drained Poisson's ratio of 0.18 and 0.31; and the permeability of  $3.64 \cdot 10^{-15}$  and  $3.29 \cdot 10^{-15} \text{ m}^4/\text{Ns}$ , respectively. The values of undrained Young's modulus were determined by measuring short period deformation of samples in the unconfined tests. A discussion on obtained results is presented.

© 2014 Elsevier B.V. All rights reserved.

## 1. Introduction

The mechanical and structural properties are important parameters that characterize suitability of hydrogel materials for bioengineering and biotechnological applications (implants, artificial muscles, scaffolds, valves, biosensors, and also materials for cartilage repair and bioreplacement) [1]. The presence of liquid phase in hydrogels significantly affects their properties because both the solid skeleton and the pore fluid can carry loads. The fluid however may flow out and this may induce changes in mechanical coefficients of the materials. Thus, experimental studies performed to determine the mechanical properties of hydrogels should be divided into two groups: tests without draining and with draining. The mechanical behavior of hydrogels without draining can be described using theory of rubber elasticity or single-phase models of viscoelastic material [2]. When draining is allowed, the mathematical modeling can be based on mixture theory [3–5] or poroelasticity models [6–8]. The model of a biphasic material was also developed in a biomechanical context independently of mixture and poroelastic theory. For example, the model of cartilage is known as KLM biphasic model [4]. The Biot theory of poroelasticity was originally developed to describe the consolidation of moist soils under applied load [6]. The Biot theory of poroelasticity and the KLM biphasic theory are equivalent when used to model the behavior of saturated poroelastic materials composed of incompressible solid and fluid constituents [9].

The parameters most frequently used to quantify the response to applied load are: drained Young's modulus ( $E_s$ ) and Poisson's ratio ( $\nu_s$ ) as well as hydraulic permeability ( $k$ ), which measures the fluid conductance in porous media. Many experimental methods for measuring mechanical properties of hydrogels have been developed. Recently, the most common methods are: tensile and extensometry tests [10,11], unconfined [3,12] and confined [4,13] compression tests and also central indentation technique [14]. The review devoted to the investigation of mechanical parameters of hydrogels reports significant differences between drained and undrained experimental conditions [15]. Moreover, frequently the experimental conditions are not precisely defined. As a result, the values of Young's modulus obtained by different methods may differ by more than 50% [16].

The aim of this paper is the identification of mechanical and hydraulic parameters of porous hydrogels based on poly(vinyl alcohol) (PVA) using creep tests. This method is based on unconfined one-dimensional compression and solution of inverse problem using poroelasticity model. The identification of three parameters: drained Young's modulus ( $E_s$ ) and Poisson's ratio ( $\nu_s$ ) as well as hydraulic permeability ( $k$ ) is carried out with the global optimization method, implemented in Matlab environment. Independently, compression tests without draining are carried out in order to determine the undrained Young's modulus of the gels.

## 2. Mathematical model of poroelastic material for unconfined creep test

As a result of loading of a porous elastic fluid-filled solid specimen a stress distribution between skeleton and pore fluid takes place. If

\* Corresponding author.

E-mail address: [kkd@ukw.edu.pl](mailto:kkd@ukw.edu.pl) (K. Kazimierska-Drobny).

boundary conditions allow the load induces deformation and changes the pore pressure along with the fluid flowing out from the sample. Then, the skeleton deformation is extended in time and macroscopically a creep is observed. There are two most often applied types of creep tests used for saturated porous materials: the confined compression tests (on the lateral surface, the skeleton deformations and outflow of fluid are limited) and the unconfined compression tests (on the lateral surface, both free deformations and fluid flow can occur). In this paper, the creep tests with unconfined compression of cylindrical hydrogel samples are used, see Fig. 1.

A cylindrical sample of hydrogel is subjected to a compressive load  $F$  along the  $z$ -axis. The load causes time evolution of axial and radial deformations, accompanied by movement of fluid outside the porous material in the direction transverse to the direction of the applied load. Taking into account that a small amount of water is also squeezed out from the loaded gel sample in the axial direction and it constitutes a fluid film lubricant one can assume that there is no friction between the sample and impermeable plates at the upper and lower base, and postulate that the hydrogel deformations in radial, as well as axial directions, and pore pressure do not depend on the coordinate  $z$ .

The mathematical model for the above formulated axisymmetric creep problem assuming a homogenous poroelastic material with incompressible matrix and liquid phases was presented in [3]. In the present paper, the most fundamental equations of the model and final solution for the axial strain are only listed. The model is based on the equilibrium equations for solid phase and fluid phase:

$$\begin{aligned} \nabla \cdot \boldsymbol{\sigma}^s + \mathbf{R} &= 0 \\ \nabla \cdot \boldsymbol{\sigma}^f - \mathbf{R} &= 0 \end{aligned} \quad (1)$$

and the mass balance equation for the system

$$n \nabla \cdot \mathbf{v}^f + (1-n) \nabla \cdot \mathbf{v}^s = 0 \quad (2)$$

where  $\boldsymbol{\sigma}^s$  and  $\boldsymbol{\sigma}^f$  are macroscopic stress tensors,  $\mathbf{v}^s$  and  $\mathbf{v}^f$  are velocity vectors for solid (s) and fluid (f) phases,  $\mathbf{R}$  denotes vector of interaction force between phases, and  $n$  is the porosity. The equilibrium Eq. (1) disregards gravity. The mass balance Eq. (2) results from combining continuity equations of phases and their incompressibility assumptions.

The constitutive equations for hydrogel material are assumed for stress tensors and interaction force as the following:

$$\begin{aligned} \boldsymbol{\sigma}^s &= -(1-n)p\mathbf{I} + \lambda_s \mathbf{e} + \mu_s \boldsymbol{\varepsilon} \\ \boldsymbol{\sigma}^f &= -np\mathbf{I} \\ \mathbf{R} &= \frac{n^2}{k} (\mathbf{v}^f - \mathbf{v}^s) \end{aligned} \quad (3)$$

where  $p$  is the pore pressure,  $\mathbf{e}$  and  $\boldsymbol{\varepsilon}$  denotes dilatation and strain tensor of solid matrix ( $\mathbf{e} = \text{tr}(\boldsymbol{\varepsilon})$ ),  $\mu_s$  and  $\lambda_s$  are Lamé constants for drained material, and  $k$  is the permeability. The viscous stress of the skeleton

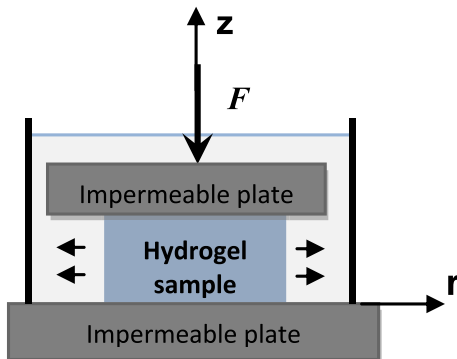


Fig. 1. Unconfined compression test of hydrogel sample.

in stress tensor is omitted due to the negligible velocity of the deformation during the process of drainage.

Eq. (3) refers to the classical model of fluid saturated poroelastic material which satisfies the Terzaghi effective stress law and the phases interact according to the Darcy's law.

The applied load  $F$  is related to the total axial stress carried by the solid matrix and the fluid:

$$\int_0^a (\sigma_{zz}^s - np_0) 2\pi r dr = F \quad (4)$$

where  $r$  denotes the radial coordinate of the cylindrical coordinate system and  $a$  is the radius of the sample.

Using the appropriate initial conditions (no initial strain of solid matrix, the pore pressure corresponding to the total load) and boundary conditions (lack of flow at sample's ends, radial component of the total stress and pore fluid pressure at lateral surface equal to zero) the solution of the creep problem is found in [3] with the help of the Laplace transform method.

The axial strain of solid matrix  $\boldsymbol{\varepsilon}$  as the function of time  $t$  is the following [3]

$$\boldsymbol{\varepsilon}(t) = -\frac{F}{E_s \pi a^2} \left[ 1 - (1-2\nu_s^2)(1-2\nu_s) \sum_{n=1}^{\infty} \frac{4}{9(1-2\nu_s)^2 \beta_n^2 - 8(1+2\nu_s)(1-2\nu_s)} e^{-\beta_n^2 \frac{H_A t}{a^2}} \right] \quad (5)$$

where  $E_s$  and  $\nu_s$  are Young's modulus and Poisson's ratio for drained material,  $H_A = \lambda_s + 2\mu_s = \frac{E_s(1-\nu_s)}{(1+\nu_s)(1-2\nu_s)}$  and  $\beta_n$  are roots of the characteristic equation

$$J_0(x) - \frac{4(1-2\nu_s)J_1(x)}{3(1-\nu_s)x} = 0 \quad (6)$$

$J_0$  and  $J_1$  are Bessel functions of the first kind of orders zero and one.

The solution given by Eq. (5) predicts creep curves, i.e. axial strain dependence over time. Two components of the strain can be distinguished: the first one, for  $t = 0^+$ , which describes the immediate deformation of a material without flow of pore fluid outside the hydrogel (undrained response to load) and the second component, for  $t > 0$ , which is responsible for the rheological processes associated with the outflow of fluid from the sample. On the basis of the first component the undrained Young's modulus can be determined assuming that Poisson's ratio amounts to 0.5. Applying the full form predicted by Eq. (5) and solving the corresponding inverse problem the drained Young's modulus and Poisson's ratio as well as the permeability of hydrogels can be determined.

### 3. Sensitivity analysis of creep model

Sensitivity analysis of poroelastic creep model is performed to determine the impact of parameters of two-phase material: drained Young's modulus ( $E_s$ ), drained Poisson's ratio ( $\nu_s$ ) and permeability ( $k$ ) on axial strains ( $\boldsymbol{\varepsilon}$ ) of a cylindrical sample assuming its diameter of  $2a = 37$  mm, and load (force) of  $F = 7$  N.

Fig. 2 shows the evolution of strains in time for three different values of Young's modulus  $E_s = 0.3, 0.45$  and  $0.6$  MPa, while Poisson's ratio  $\nu_s = 0.3$  and permeability  $k = 2 \cdot 10^{-15} \text{ m}^4/\text{Ns}$ .

The results show that the increase in Young's modulus results in a systematic shift of deformation along the vertical axis. The observed behavior is associated with a reduction of the value of the initial strain.

Fig. 3 shows the time evolution of axial strain for three values of Poisson's ratio:  $\nu_s = 0.3, 0.35$  and  $0.4$ , while the Young's modulus  $E_s = 0.3$  MPa and permeability  $k = 2 \cdot 10^{-15} \text{ m}^4/\text{Ns}$ .

The simulations indicate that Poisson's ratio affects mostly the value of the initial deformation, and the greater the  $\nu_s$  the greater the value of

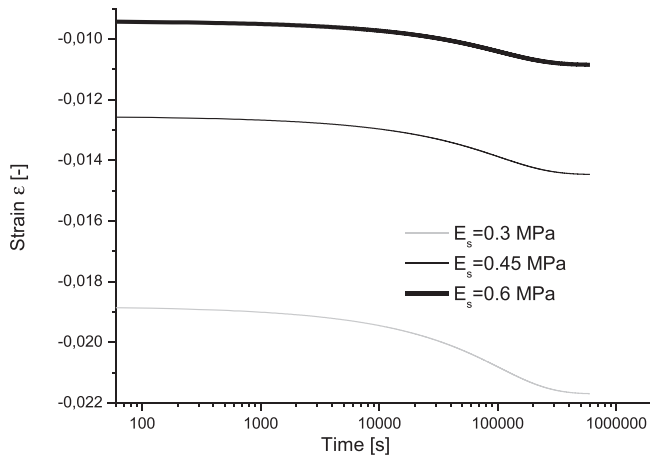


Fig. 2. Evolution of axial strain for different values of drained Young's modulus.

the initial strain is observed. For a sufficiently long time the value of strain reaches the same level, independently of the value of Poisson's ratio.

Fig. 4 shows the time evolution of axial strain for three different values of permeability  $k = 2 \cdot 10^{-15}$ ,  $4 \cdot 10^{-15}$  and  $6 \cdot 10^{-15} \text{ m}^4/\text{Ns}$ , while Young's modulus  $E_s = 0.3 \text{ MPa}$  and Poisson's ratio  $\nu_s = 0.3$ .

The value of permeability determines the time when the final value of deformation is achieved, but does not affect the value of the initial and final strains. This means that the permeability is responsible for the rate of poroelastic creep.

#### 4. Materials and methods

Poly(vinyl alcohol) (PVA, Mw = 146 000–186 000 g/mol; degree of hydrolysis 99%, Du Pont, Elvanol) hydrogels were prepared by freezing–thawing according to the procedure described elsewhere [11]. PVA aqueous solutions were prepared at two concentrations: 22wt.% and 25 in an oven at 90° during 12h. Prepared solutions were placed in cylindrical Teflon® molds (40 mm diameter, 100 mm height). Samples were subjected to freezing at  $-18^\circ$  for 12 h and thawing at  $18^\circ$  for 12 h for 4 cycles. During this process, water acts as a porophor. The cylinders (about 100 mm in height) were cut into homogeneous samples avoiding visible defects (pores) at their circumferential surface. This resulted in different heights of samples. The difference in diameters of samples was caused by different shrinking of hydrogels. The sample size of PVA hydrogels taken for mechanical tests is presented in Table 1.

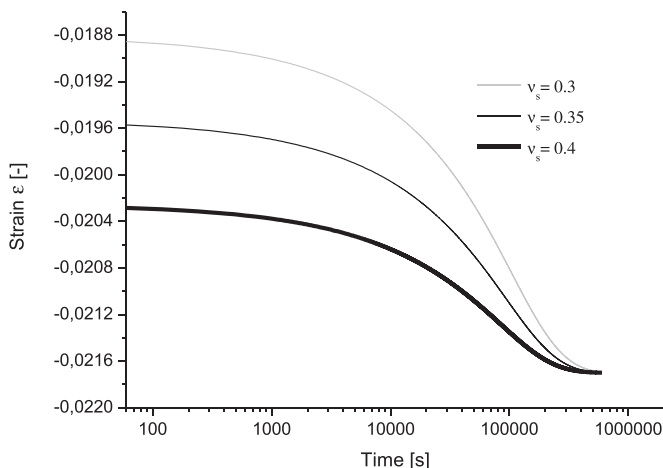


Fig. 3. Evolution of axial strain for different values of drained Poisson's ratio.

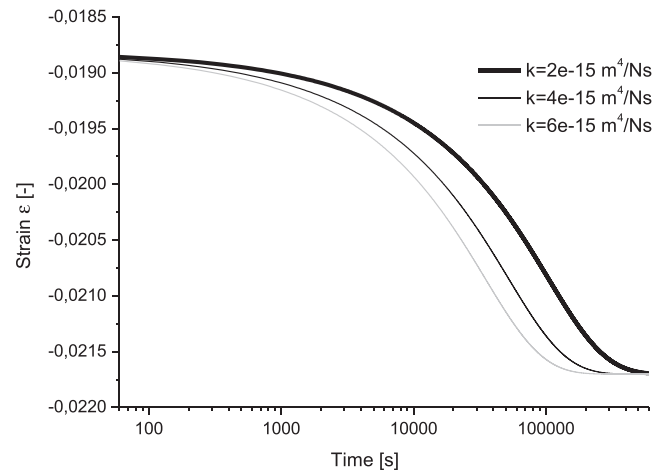


Fig. 4. Evolution of axial strain for different values of permeability.

The measurements were done using the experimental system shown in Fig. 5. The system consists of the following elements: temperature-stabilizing measurement chamber with loading system and ultrasonic transducer, ultrasonic testing apparatus OPTEL OPBOX 01/100, PC, and thermostat (HAAKE DC 30/DL30), which stabilizes temperature of samples during the test. All measurements were conducted at 25 °C.

Samples of hydrogels were tested in the chamber shown in Fig. 5b. The chamber consists of two rings made from PMMA placed between stainless steel plates. The internal ring has an inner diameter of 40 mm and contains a sample of hydrogel in water. The external ring has an inner diameter of 70 mm and the space between the rings is filled with liquid, which stabilizes the temperature of samples. The samples are loaded axially by weights placed on an intermediate structural element and via an impermeable rigid disc which can freely move vertically. For each study a preloading force 6 N is applied to fix the positions and shape of samples.

The displacement (settlement) of sample under load is continuously recorded by time of flight method using ultrasonic testing system and pulse signals. The transducer with the main frequency 5 MHz is fixed to the upper plate of the chamber and its face is immersed in liquid (see Fig. 5b). The ultrasonic signals are registered every 60 s and transferred to PC. Then, the data are processed offline in order to determine settlements using the correlation method. The measurement chamber is linked with thermostat which stabilizes temperature during the tests. In the creep tests samples of hydrogels are subjected to constant load 11.09 N.

## 5. Results

### 5.1. Creep tests

Examples of denoised creep curves for studied PVA hydrogels under constant load 11.09 N are shown in Fig. 6.

The deformations recorded in the creep test have two characteristic components: (i) the deformation observed immediately after applying the load, which takes place without flow of liquid from hydrogel material (undrained deformation) and (ii) the deformation being the result

Table 1  
Basic characteristic of PVA hydrogel samples.

Concentration of polymer PVA [%]	Sample height H [mm]	Sample diameter d [mm]
25% PVA	12.47 ± 0.07	37.75 ± 0.18
22% PVA	16.02 ± 0.14	36.80 ± 0.13

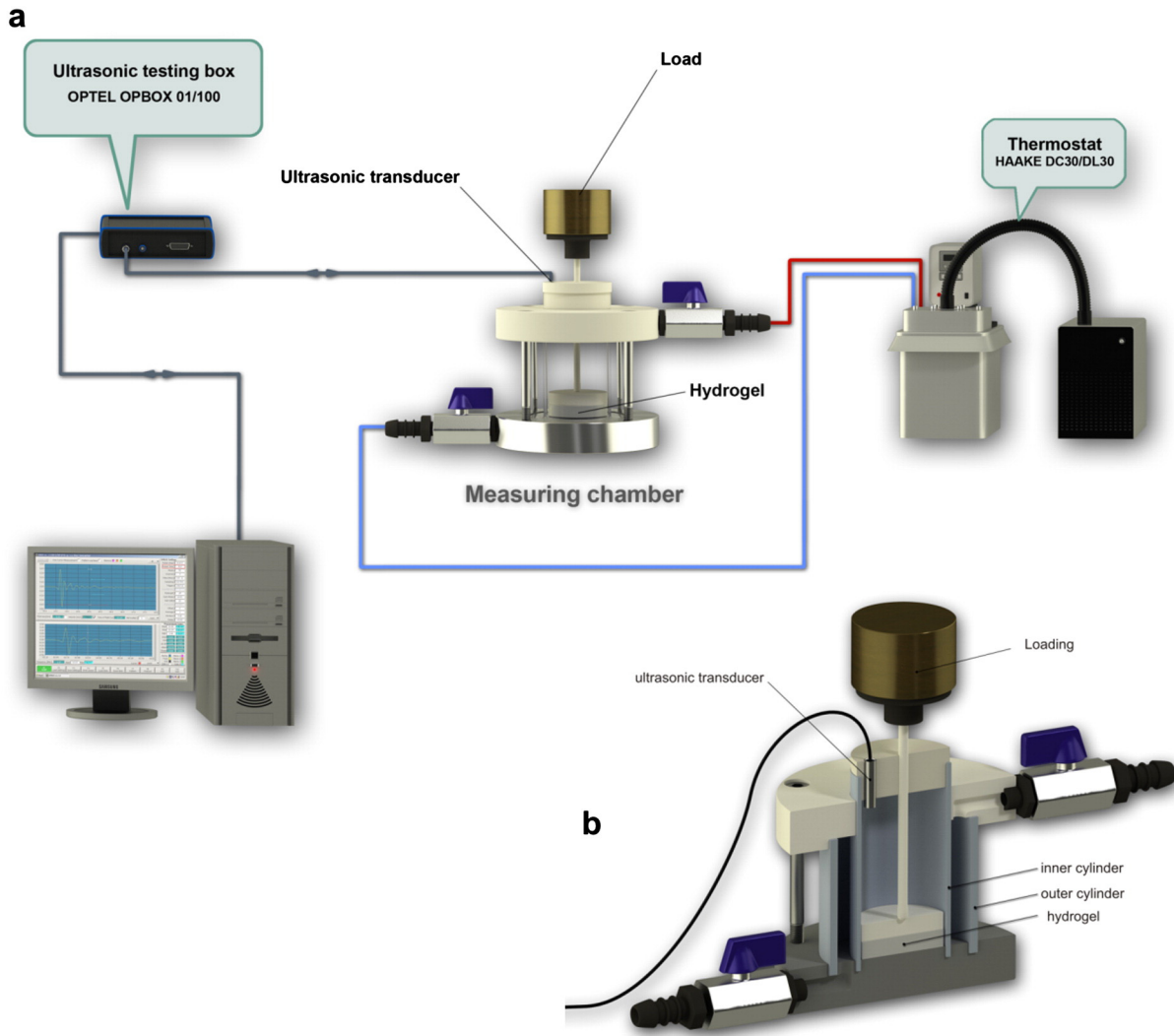


Fig. 5. The schematic of the applied experimental system (a) and cross-section through the measurement chamber (b).

of poroelastic creep, accompanied by outflow of fluid from the hydrogel. The maximum strain recorded in the creep test for 22% of the PVA material is approximately 1.4% and for 25% of the PVA material it amounts approximately 1.1%.

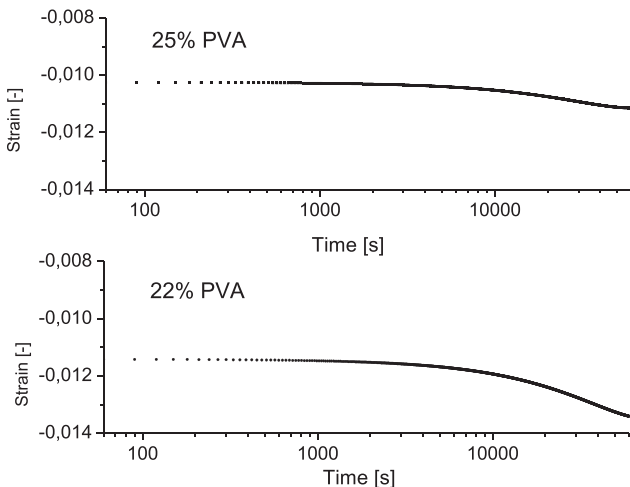


Fig. 6. Results of unconfined creep tests of the studied PVA hydrogels.

It should be noticed that within time interval of the experiments the deformation does not reach a constant value. Results reported in literature show similar behavior for PVA hydrogels [8,17] as well as for other polymeric materials, e.g. pHEMA [18] and agar hydrogel [19]. This phenomenon is probably associated with the second creep mechanism based on the evolution of internal structure of polymers [8,17–19].

## 5.2. Identification of poroelastic constants

Based on the obtained experimental data of the time evolution of strain in the creep tests and the appropriate solution of the poroelasticity model the identification problem is solved in order to determine three parameters: drained Young's modulus ( $E_s$ ), drained Poisson's ratio ( $\nu_s$ ) and permeability ( $k$ ). The procedure of identification uses Genetic Algorithm optimization method implemented in Matlab environment. The average results are given in Table 2. Additionally, Table 2 contains the results for Young's modulus  $E$  determined from undrained tests (see Appendix A).

The results of identification show that the drained Young's moduli ( $E_s$ ) obtained from creep tests are lower than the undrained Young's modulus ( $E$ ) for two different kinds of hydrogels. The Young's moduli for both testing conditions (undrained and drained ones) are higher for hydrogels with 25% PVA. The Young's moduli obtained from the performed small strain unconfined compression tests with the maximum axial strain of about 1.4% are comparable with results from other small

**Table 2**  
Values of mechanical constants and permeability of PVA hydrogels.

Material	Creep test			Undrained test
	$E_s$ [MPa]	$\nu_s$ [–]	$k \cdot 10^{-15}$ [m <sup>4</sup> /Ns]	$E$ [MPa]
25% PVA	0.902 ± 0.030	0.31 ± 0.03	3.29 ± 1.16	0.924 ± 0.037
22% PVA	0.715 ± 0.046	0.18 ± 0.03	3.64 ± 2.05	0.885 ± 0.037

strain tests and significantly lower than results from large deformation tests reported in the literature. For example the compressive Young's moduli for 20%, 30% PVA hydrogels after 6 cycles of freezing and thawing determined from the initial portion of stress–strain curve (1–5% strain) amount 0.241; 0.678 MPa respectively [20]. In turn, the results from tensile tests for 25% PVA hydrogel at 60% strain level [11] give the Young's modulus ranged from 7.23 to 14.09 MPa.

The values of drained Poisson's ratio ( $\nu_s$ ) for the tested materials are significantly below the value for incompressible material (0.5). The drained Poisson's ratio is also higher for hydrogel samples with 25% PVA. Both values of  $\nu_s$  are also comparable with the values determined for other hydrogels presented in the literature, see e.g. 0.20 for 30% PVA [8], 0.10 for bovine kneecap [12], 0.30 for pHEMA-MAA [21] and also 0.30 for agar hydrogel [22].

The values of permeability of hydrogels with 22% PVA and 25% PVA are similar and amount to around  $3.5 \cdot 10^{-15}$  [m<sup>4</sup>/Ns]. Thus, any significant influence of concentration of polymer on the value of the coefficient is not observed. The values are close to permeability found for other hydrogel materials produced on the basis of PVA, like for example 10% PVA–PVP  $k$  is from 19 to 33  $\cdot 10^{-15}$  m<sup>4</sup>/Ns [23].

Following the assumptions of poroelasticity theory the drained and undrained elastic moduli of isotropic porous media can be related assuming equality of shear moduli for both loading conditions, i.e.  $\mu = \mu_s$  [3]. Thus, calculating drained shear modulus  $\mu_s$  from  $E_s$  and  $\nu_s$  ( $\mu_s = E_s/2(1 + \nu_s)$ ) and assuming incompressibility of undrained material ( $\nu = 0.5$ ) we can determine the undrained Young's modulus as  $E = 2\mu(1 + \nu) = 3\mu = 3\mu_s$  [3]. Since the values of  $\mu_s$  for tested hydrogels H\_4A and H\_5A are: 0.34 MPa and 0.30 MPa, the calculated undrained Young's moduli are: 1.03 and 0.96 MPa, respectively. The obtained values of  $E$  are about 10% higher than the values found directly from unconfined compression tests without draining (Appendix A) and are presented in Table 2.

Fig. 7 shows plots which compare theoretical and experimental creep curves for the studied PVA materials while the results of simulations were derived assuming the average values of estimated parameters (given in Table 2 constants  $E_s$ ,  $\nu_s$  and  $k$ ).

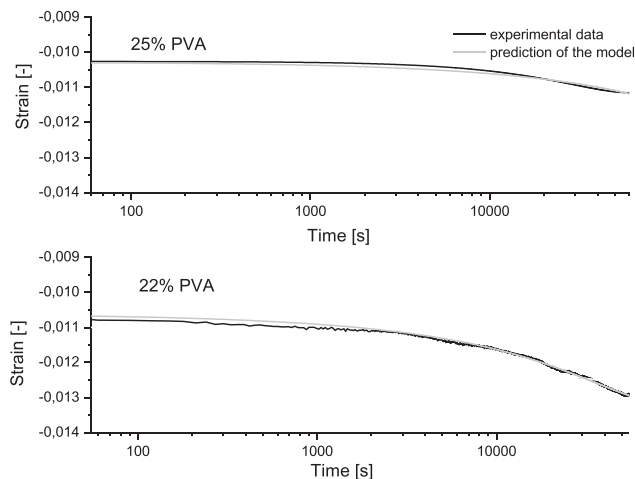


**Fig. 7.** Comparison of experimental creep curves with model predictions.

The agreement of the experimental and theoretical curves seems to be satisfactory although discrepancies are visible. The possible sources of misfit are fluctuations of temperature, denoising procedure or limitations of the applied model.

## 6. Conclusions

The purpose of this paper was the identification of mechanical and hydraulic properties for poly(vinyl alcohol) hydrogels with two concentrations of PVA (22 and 25%) using creep tests. This method was based on unconfined one-dimensional compression and solution of inverse problem using poroelasticity model. The identification of three parameters: drained Young's modulus ( $E_s$ ) and Poisson's ratio ( $\nu_s$ ) as well as hydraulic permeability ( $k$ ) was carried out with the global optimization method, implemented in Matlab environment. Independently, the one-dimensional compression tests without draining were carried out in order to determine the undrained Young's moduli of the gels. The estimated values of the Young's moduli for 22% PVA and 25% PVA with draining are less than 1 MPa and the values roughly agree with values obtained by other researchers for the study of similar materials. Moreover the values of Young's moduli with draining are less than Young's moduli without draining which confirms the biphasic nature of the materials and also a significant contribution of water in the transmission load during the creep test. For both kinds of tests the Young's moduli were higher for the materials with higher PVA concentration. The drained Poisson's ratio was significantly less than 0.5. This also exhibits the two-phase nature of the studied hydrogels. The value of hydraulic permeability is not dependent on concentration of PVA (for 22 and 25%). It amounts to about  $3.5 \cdot 10^{-15}$  m<sup>4</sup>/Ns and is close to the values for other hydrogel materials produced on the basis of PVA.

The obtained results indicate that hydrogels have similar mechanical and hydraulic properties as some connective tissues and can therefore be used as for example bio-replacement materials in the regeneration of cartilage. For such bio-engineering applications studies of chemo-mechanical behavior of PVA hydrogels are carried out taking into account the presence of salts in fluid. The research which will be reported soon is focused on determination of parameters of the coupled transport (forced by gradients of pore pressure and concentration) and the influence of the saline environment on the deformation of hydrogel. Since our previous studies of PVA hydrogels proved high thermosensitivity of the materials appropriate tests and modeling efforts are undertaken.

## Acknowledgments

This work was partially supported by the National Science Centre in Poland under grant UMO-2013/11/B/ST8/03589.

## Appendix A. Unconfined compression tests without draining

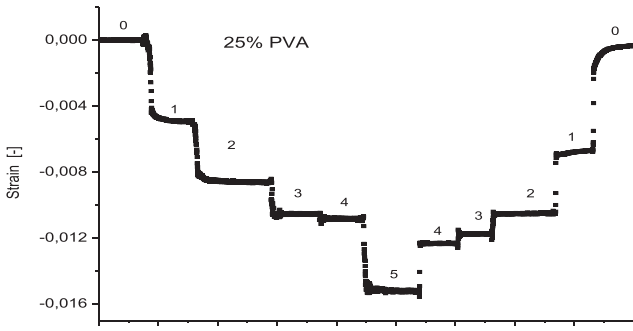
In order to estimate the undrained Young's modulus of studied materials series of the unconfined compression tests without draining were performed. The tests were carried out by applying short periods of loading or unloading of upper base of cylindrical samples with simultaneous registration of their displacements. Although the lateral surface of samples was not insulated, low permeability of studied hydrogel materials ensures that the undrained conditions are met.

Fig. A.1 shows the changes of strain for loading and unloading of hydrogel samples with initial concentration of 25% PVA.

The maximum strains for 25% PVA were about 1.5% for the load 18.4 N. Similar results for hydrogels with initial concentration of PVA of 22% are shown in Fig. A.2. The maximum strains for 22% PVA were about 2%.

The graphs shown in Fig. A.3 present stress–strain dependence for the whole loading history of the studied hydrogels.

The results show that in the investigated range of undrained compression the stress–strain dependencies are approximately linear.



**Fig. A.1.** Strain variation for loading and unloading processes of hydrogels with 25% of PVA loads: 1–4.3 N, 2–8.6 N, 3–10.6 N, 4–11.3 N, and 5–18.4 N.

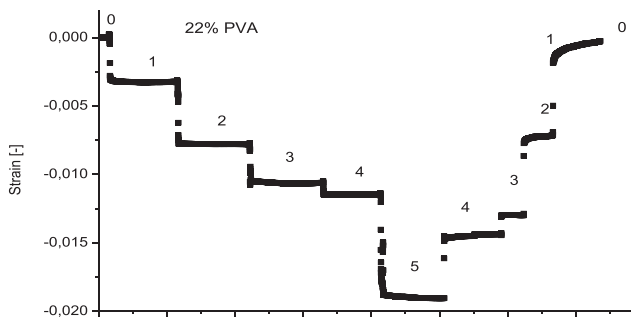


**Fig. A.2.** Strain variation for loading and unloading processes of hydrogels with 22% of PVA loads: 1–4.3 N, 2–8.6 N, 3–10.6 N, 4–11.3 N, and 5–18.4 N.

The results are used to estimate the undrained Young's modulus of hydrogels, presented in Table 2. In the case of 22% PVA a small hysteretic effect is observed, i.e. for the same stress level the values of strains are different for the process of loading and unloading.

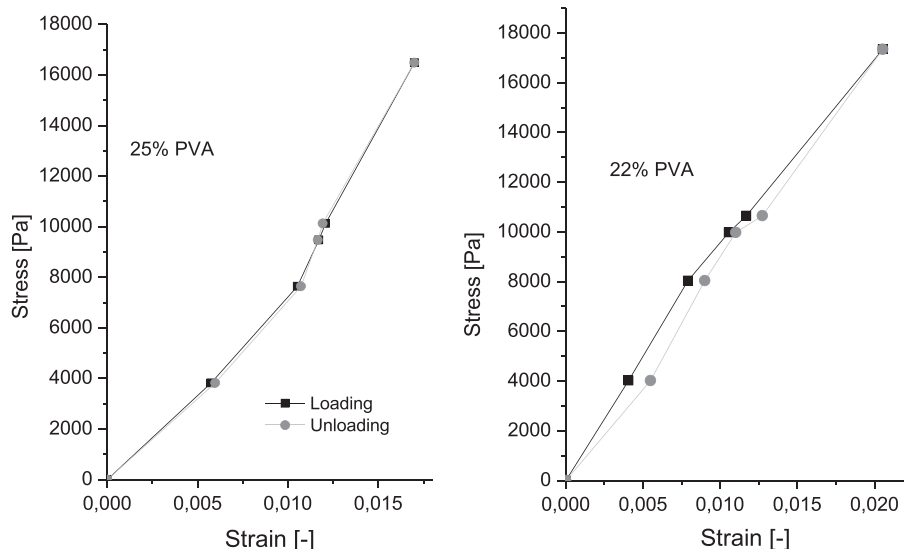


**Fig. A.3.** Stress–strain dependence for loading and unloading of studied hydrogels.

**References**

- [1] Ch.M. Hassan, N.A. Peppas, Structure and applications of poly(vinyl alcohol) hydrogels produced by conventional crosslinking or by freezing/thawing methods, *Adv. Polym. Sci.* 153 (2000) 37–65.
- [2] K.S. Anseth, Ch.N. Bowman, L. Brannon-Peppas, Mechanical properties of hydrogels and their experimental determination, *Biomaterials* 17 (1996) 1647–1657.
- [3] C.G. Armstrong, W.M. Lai, V.C. Mow, An analysis of the unconfined compression of articular cartilage, *J. Biomed. Eng.* 106 (1984) 165–173.
- [4] V.C. Mow, S.C. Kuei, W.M. Lai, C.G. Armstrong, Biphasic creep and stress relaxation of articular cartilage: theory and experiments, *J. Biomech. Eng. Trans. ASME* 102 (1980) 73–84.
- [5] K.L. Spiller, S.J. Laurencin, D. Charlton, S.A. Maher, A.M. Lowman, Superporous hydrogels for cartilage repair: evaluation of the morphological and mechanical properties, *Acta Biomater.* 4 (2008) 17–25.
- [6] M.A. Biot, General theory of three-dimensional consolidation, *J. Appl. Phys.* 12 (1941) 155–164.
- [7] M. Kaczmarek, *Mechanics Saturated Chemically Sensitive Materials*, Publisher University of Bydgoszcz, Bydgoszcz, 2001. (in polish).
- [8] P. Silva, S. Crozier, M. Veidt, M.J. Pearcy, An experimental and finite element poroelastic creep response analysis of an intervertebral hydrogel disc model in axial compression, *J. Mater. Sci. Mater. Med.* 16 (2005) 663–669.
- [9] G.P. Berry, J.C. Bamber, C.G. Armstrong, N.R. Miller, P.E. Barbone, Towards an acoustic model-based poroelastic imaging method: I. Theoretical foundation, *Ultrasound Med. Biol.* 32 (4) (2006) 547–567.
- [10] J.L. Drury, D.J. Mooney, Hydrogels for tissue engineering: scaffold design variables and applications, *Biomaterials* 24 (2003) 4337–4351.
- [11] M. El Fray, A. Pilaszkiwicz, W. Swieszkowski, K. Kurzydowski, Chemically and physically crosslinked poly(vinyl alcohol) hydrogels for cartilage repair, *E-Polymer* P-013 (2005) 1–6.
- [12] M.R. DiSilvestro, J.-K.F. Suh, A cross-validation of the bi-phasic poroviscoelastic model of articular cartilage in unconfined compression, indentation and confined compression, *J. Biomech.* 34 (2001) 519–525.
- [13] E. Behraves, M.D. Timmer, J. Lemoine, A.K. Liebschner, A. Mikos, Evaluation of the in vitro degradation of macroporous hydrogels using gravimetry, confined compression testing and microcomputed tomography, *Biomacromolecules* 3 (2002) 1263–1270.
- [14] R.K. Korhonen, M.S. Laasanen, et al., Comparison of the equilibrium response of articular cartilage in unconfined compression, confined compression and indentation, *J. Biomech.* 35 (2002) 903–909.
- [15] K. Kazimierska-Drobny, *Simulation of Chemo-mechanical Processes in Porous Hydrogels and Identification of Parameters*, IPPT PAN, Warszawa, 2011. (in Polish).
- [16] S. Gabler, J. Stampfl, T. Koch, S. Seidler, G. Schuller, H. Redl, Determination of the viscoelastic properties of hydrogels based on polyethylene glycol diacrylate (PEG-DA) and human articular cartilage, *Int. J. Mater. Eng. Innov.* 1 (2009) 3–21.
- [17] K. Liu, B. Thomas, C. Fryman, J. Bischoff, T. Ovaert, J. Mason, Optimization-based inverse element analysis for material parameter identification of biphasic viscoelastic hydrogel, *Proceedings of the ASME 2008 Summer Bioengineering Conference*, Florida USA, 2008.
- [18] A. Gloria, F. Causa, R. De Santis, P.A. Netti, L. Ambrosio, Dynamic-mechanical properties of a novel intervertebral disc prosthesis, *J. Mater. Sci. Mater. Med.* 18 (2007) 2159–2165.

- [19] D.G. Strange, T.L. Fletcher, T. Tonsomboon, H. Brawn, X. Zhao, M. Oyen, Separating poroviscoelastic deformation mechanism in hydrogel, *Appl. Phys. Lett.* 102 (031913) (2013) 1–4.
- [20] J.L. Holloway, K.L. Spiller, A.M. Lowman, G.R. Palmese, Analysis of the in vitro swelling behavior of poly(vinyl alcohol) hydrogels in osmotic pressure solution for soft tissue replacement, *Acta Biomater.* 7 (2011) 2477–2482.
- [21] S.J. Lee, G.R. Bourne, X. Chen, W.G. Sawyer, M. Sarntinoranont, Mechanical characterization of contact lenses by microindentation. Constant velocity and relaxation testing, *Acta Biomater.* 4 (2008) 1560–1568.
- [22] J.E. Olberding, J.-K.F. Suh, A dual optimization method for the material parameter identification of a biphasic poroviscoelastic hydrogel: potential application to hypercompliant soft tissues, *J. Biomech.* 39 (2006) 2468–2475.
- [23] P. Chiarelli, A. Lanata, M. Carbone, Acoustic waves in hydrogels: a bi-phasic model for ultrasound tissue-mimicking phantom, *Mater. Sci. Eng. C* 29 (2009) 899–907.